LAWRENCE
LIVERMORE
NATIONAL
LABORATORY

LLNL-JRNL-562678

A Snowflake Divertor: Solving a Power Exhaust Problem for Tokamaks

D. D. Ryutov, R. H. Cohen, T. D. Rognlien, M. V. Umansky

June 28, 2012

Plasma Physics and Controlled Fusion

Disclaimer

LLNL-JRNL-562678

A snowflake divertor: solving a power exhaust problem for tokamaks

D D Ryutov, R H Cohen, T D Rognlien, and M V Umansky

Lawrence Livermore National Laboratory, Livermore, CA 94551, USA

Abstract. Handling the heat and particle exhaust in large tokamaks is one of the most challenging problems of fusion research. The concept of a snowflake (SF) divertor offers a possible path to reducing both steady-state and intermittent heat loads on the divertor plates to an acceptable level. The most important feature of a SF divertor is the presence of a large zone of a very weak poloidal magnetic field around the poloidal field (PF) null. This paper summarizes recent progress in the theory of a snowflake divertor. Qualitative explanation of a variety of new features characteristic of a SF divertor is provided based on simple scaling relations. The main part of the paper is focused on the spreading of the heat flux by curvature-driven convection near the poloidal field null. References to experimental results from the NSTX and TCV tokamaks are provided.

1. Introduction

A significant fraction (~ 20%) of the power released in the burning plasma core of a reactor-tokamak will have to be accommodated on the surfaces facing the plasma [1, 2]. This will be accomplished by creating a magnetic divertor configuration with a poloidal field (PF) null (or two nulls). The presence of the null leads to formation of the magnetic separatrix, which separates the closed magnetic flux surfaces in the confinement zone from the open flux surfaces beyond the confinement zone. After crossing the separatrix, the plasma is lost to the material surfaces that intersect the open field lines. Because the parallel plasma transport along the field lines is much faster than perpendicular transport, the plasma layer outside the separatrix, the so-called scrape-off layer (SOL), is quite narrow compared to the plasma minor radius. The presence of the separatrix allows control of the global plasma shape and prevents the plasma from contacting and damaging the first wall of the confinement vessel. The plasma losses are "diverted" away from the walls to the thermally and mechanically hardened surface of the divertor.

In order to increase the longevity of the divertor components, it is desirable to keep the heat flux at the absorbing surfaces as low as possible. In this paper, we describe one of the potential solutions of this problem, the so-called "snowflake divertor" [3]. We provide a broad assessment of the concept using scaling relations and order-of-magnitude estimates. This approach allows us to discuss all essential features of this configuration in a relatively short paper. We do not discuss in detail experiments on two tokamaks, NSTX and TCV, where this configuration has been studied, but briefly summarize the results and provide references to relevant papers. Note that the summary of these experiments to date will appear in the Proceedings of the 10th International Conference on Plasma-Surface Interactions, Aachen, May 2012 [4].

There exists a broad range of ideas related to possible improvements of the divertor operation: a radiative divertor (Ref. [5] and references therein), a puff-and-pump divertor [6], a super-X divertor based on increasing the major radius of the strike-point [7], to name a few; see also the ARIES study [2]. In this paper, we focus on the snowflake divertor.

One of the most important observations made in the first publications on the snowflake divertor [3, 8] was that this configuration can be created by the poloidal field (PF) coils situated at large distances from the desired position of the null. This circumstance is still sometimes missed in the assessment of the potentialities of a snowflake divertor, and the perceived need of PF coils inside toroidal field (TF) coils is mentioned as its drawback (see, e.g., Ref. 9).

The characteristic scale for the required distance is the size of the confinement zone inside the separatrix, which will be a few meters in the energy-producing facilities. This provides enough space to install the PF coils not only outside the blanket, but also outside the TF coils. The PF coil location outside TF coils is assumed in design studies [10, 11] of future tokamaks with SF divertors.

The aforementioned misconception may be related to the fact that the SF configuration can also be created by the coils situated very near the separatrix, as is the case for the spherical torus NSTX [12]. But this example just shows the flexibility of the SF configuration, not that it *requires* that the coils be close to the magnetic null.

In general, detailed experiments performed on two tokamaks, TCV (Lausanne) and NSTX (Princeton) [12-18] have shown that the transition to a snowflake configuration on some of the existing devices is possible even without any modifications of the hardware. The H-mode is found to be fully compatible with this configuration, and the plasma parameters usually improved compared to the standard case. Implementation of the snowflake did not lead to any significant reduction of the volume of the confined plasma.

2. Geometrical features

The idea behind the snowflake configuration is to make not only the poloidal magnetic field, but also its first spatial derivatives zero at a chosen point. The poloidal magnetic field strength near the snowflake (SF) null varies as r^2, where r is the distance from the null. The structure of the flux surfaces in the vicinity of the null is governed by the 2D Laplace equation for the flux function Φ: $(1/r)(\partial/\partial r)(r\partial\Phi/\partial r)+(1/r^2)(\partial^2\Phi/\partial\varphi^2)=0$ where φ is a polar angle in the poloidal plane. For the magnetic field varying as r^2, the flux function varies as r^3, this leading to the following equation determining the angular dependence of Φ: $\partial^2\Phi/\partial\varphi^2+9\Phi=0$, with a solution $\Phi\propto\cos[3(\varphi-\varphi_0)]$, where the angle φ_o depends on the orientation of the coordinate frame in the poloidal plane. This solution leads to a characteristic hexagonal shape of the separatrix, reminiscent of a snowflake (Fig. 1). Note that for the standard divertor, with the first-order null, one has $\Phi\propto r^2$, $\partial^2\Phi/\partial\varphi^2+4\Phi=0$, and $\Phi\propto\cos[2(\varphi-\varphi_0)]$, with the four branches of the separatrix intersecting at a right angle.

The poloidal field strength $B_p=|\boldsymbol{B}_p|$ near the snowflake null can be related to the poloidal field in the midplane, B_{pm}, as

$$B_p = C_1 B_{pm}(r/a)^2 \sim B_{pm}(r/a)^2 \ , \qquad (1)$$

where r is the distance from the null, a is the minor radius, and the numerical coefficient C_1 of order one depends on the details of the global geometry. In the further estimates and scaling relations, we set $C_1=1$.

Each flux surface can be characterized by its distance Δ from the separatrix in the midplane. Flux conservation then implies that the distance r from this surface to the null in the divertor region (Fig. 1) is related to Δ by

$$r \sim a\left(\Delta / a\right)^{1/3} \qquad (2)$$

where all the numerical coefficients are taken to be of order 1. Equations (1) and (2) are the basic scaling relations that determine the properties of a snowflake.

Analogously, for the standard X-point configuration, one has:

$$B_p = C_2 B_{pm}(r/a) \sim B_{pm}(r/a)\,,\; r \sim a\left(\Delta / a\right)^{1/2}\,. \qquad (3)$$

3. Effect on plasma confinement and exhaust

The distinct features of the snowflake configuration from the standpoint of plasma confinement and exhaust stem from the presence of a region of very low poloidal magnetic field near the magnetic null. The consequences are manifold.

First, due to the much lower PF strength, the flux expansion near the null becomes significantly higher. This effect can be directly used to reduce heat flux in "open" divertors, of the type used in the NSTX spherical torus. In this case, if the divertor floor is close to the null point, one can fully exploit this stronger flux flaring. Such regimes have been successfully realized on NSTX, where an easier transition to the detached plasma state and reduced amount of impurities in the core have been recorded [12, 17, 18]. According to Eqs. (2)-(3), the flux expansion for a=200 cm and Δ=0.5 cm is 2-3 times larger for the SF divertor than for the standard one.

Second, the presence of a large zone of weak field leads to an increased connection length between the midplane and the target. The connection length can be written as

$$L = \int_1^2 \frac{\sqrt{B_T^2 + B_P^2}\, d\ell}{|B_P|}\,, \qquad (4)$$

where the integration is performed along the poloidal field line, with length element $d\ell$, and the numbers "1" and "2" denoting the points in the midplane and on the divertor plate locations, respectively. The presence of a small factor $|B_P|$ in the denominator leads to a significant increase of the connection length compared to the standard divertor for flux surfaces with the same distance Δ from the separatrix in the midplane [3, 8], Cf. Eqs. (2)-(3). For the practically important case of small Δ, the connection length scales as $\ln(a/\Delta)$ for the standard divertor and as $(a/\Delta)^{1/3}$ for the snowflake divertor. The increased length causes dilation of the ELM (Edge Localized Mode) heat pulse on its way from the midplane to the strike point [19].

Third, the specific volume of the flux-tube becomes significantly larger. For two nearby flux surfaces enclosing a small poloidal flux $\delta\Phi$, the volume of the annulus is

$$\delta V = \int_1^2 2\pi R \frac{\delta\Phi}{|B_P|} d\ell \qquad (5)$$

with the specific volume being $\delta V / \delta\Phi$. For a tokamak with a standard (not too small) aspect ratio, the major radius and toroidal field experience only modest variation between the midplane and strike point, so that one can approximately assume that B_T and R are constant along the integration path; also one has $B_T >> B_p$. With these assumptions, $L \approx B_T \int_1^2 d\ell / |B_P|$, and $\delta V / \delta\Phi = (2\pi R / B_T) L$, so that the specific volume is proportional to the connection length. Therefore, the specific volume of flux tubes in the vicinity of the separatrix for the snowflake is larger than for the standard divertor. The specific volume diverges faster for the snowflake than for the standard divertor, $(a/\Delta)^{1/3}$ vs. $\ln(a/\Delta)$. The increased volume means that the radiation power from the low poloidal field zone will significantly increase for the snowflake, especially near the separatrix. This factor should have a favorable impact on divertor performance. Indications that this effect is indeed present have been found in UEDGE simulations, Ref. [20].

Fourth, the magnetic safety factor q just inside the separatrix increases substantially due to the contribution of the low field region. It diverges as $q \propto \Delta^{-1/3}$ vs a logarithmic divergence for the standard divertor. Larger q variation, in turn, means a significant increase of the magnetic shear in the pedestal region that may lead to improved pedestal stability [21 - 23].

Fifth, the weakness of the poloidal field leads to substantially increased prompt ion losses through the area surrounding the magnetic null. The prompt losses occur for trapped ions with turning points in the vicinity of the magnetic null [24]. As the poloidal velocity of these ions contains a factor B_P/B_T, their residence time in the vicinity of the null is very long. Then, for the direction of the toroidal drift towards the null, these ions cross the separatrix and are lost. As was shown in Ref. [25] the area around the null-point affected by this mechanism has a size

$$d \sim a\varepsilon^{2/5};\ \varepsilon = \frac{\rho_i}{a}\frac{B_T}{B_{pm}}\sqrt{\frac{a}{R}}, \qquad (6)$$

where ρ_i is the ion gyroradius. For the standard null the loss zone is smaller, $d \sim a\varepsilon^{2/3}$. For most existing tokamaks, the difference between this estimate and Eq. (6) is of order of a factor of 3.

As this loss mechanism affects only the ions, it is expressly non-ambipolar and, as pointed out in Ref. [26] it can control the radial electric field in the pedestal region, thereby controlling the velocity shear and, potentially, the ELM activity. Further analysis is needed to quantify the possible effect on ELMs, but it is certain that the effect will be stronger for the snowflake.

Sixth, the strong local shearing of the magnetic field also leads to changed dynamics of the plasma blob filaments [27] on the *open* field lines: the blob connectivity to the divertor plate is reduced due to the stronger shear [28].

To summarize this section: the SF geometry has a strong impact on a number of processes occurring in edge plasma, on both the closed and open flux surfaces. For the facilities where a transition from the first-order null to the second-order null is possible this provides an opportunity for studies of the processes affecting the plasma behavior at the edge. Most of the effects associated with snowflake are favorable in terms of possible control over the pedestal region and heat flux to the divertor plates.

4. The proximity condition

As was realized in the first assessments of a snowflake [3, 8], an exact snowflake configuration is topologically unstable: if the PF coil current is even slightly different from the exact value, the second-order null is split in two first-order nulls (Fig. 2). The distance D between the nulls is small as long as the current is close to the exact value. The merging of the nulls can serve as a basis for a control algorithm directed towards the generation of a snowflake (or near-snowflake), Refs. 29, 30.

It is obvious that, if the distance D is "small-enough," the properties of the configuration are close to those of the exact snowflake. The question is how small is "small-enough." In this section we provide a systematic assessment of this issue. As it turns out, the answer depends on which effect one is concerned with (flux flaring, prompt ion losses, etc.).

As shown in Ref. [29], if D is significantly smaller than the minor radius a, then the field structure at a distance r satisfying $D<r<a$ becomes essentially indistinguishable from an "exact snowflake", with six branches of the separatrix emerging from the zone where two nulls are situated. One has to zoom in on the area of two split nulls to notice the difference. Then, if the effects one is concerned with are determined by distances exceeding D, the configuration can be considered a snowflake, with the scalings (1) and (2) being applicable.

Now we formulate this condition for each of the effects mentioned in Sec. 3.

For the flux expansion effect near the null, D should be less than the projected thickness of the midplane SOL width determined by Eq. (2):. $D < D_{expansion} \equiv a\left(\Delta / a\right)^{1/3}$ If one is interested in some narrower sub-structure near the separatrix, one has to substitute its midplane width instead of Δ in this relation. The same proximity condition holds when one has to evaluate three other geometrical parameters: the connection length (4), the specific volume (5), and the safety factor q.

For the flux surfaces inside the separatrix, the parameter Δ is the distance from the separatrix in the midplane. For the problem of prompt ion losses, D must be smaller than the distance d, Eq. (6), determining the volume affected by this loss channel, $D < D_{prompt} \equiv a\varepsilon^{2/5}$. For blob connectivity, D must be smaller than the distance of the filament to the nulls. Finally, the effects of a pressure-driven convection on open field lines discussed in the next section are unaffected by finite D if the radius of the zone where β_p is greater than unity exceeds D, $D < D_{\beta_p} \equiv r^*$, where r^* is introduced in the next section (Eq. (7)). These results are summarized in Table 1.

5. Curvature-driven plasma convection

The smallness of the poloidal field near the second-order null leads to the appearance of a zone where the plasma pressure is much higher than the poloidal magnetic pressure. This zone can be considered as that where the plasma equilibrium has to be provided by the toroidal field only (the poloidal field is too small). However, it is well-known (e.g., [31]) that toroidal field alone can only support equilibria where the pressure is a function of the major radius alone, which is incompatible with the plasma pressure distribution near the PF null, where the pressure certainly decreases in the downward direction.

As was pointed out in Ref. 32, the lack of an equilibrium leads to the onset of the plasma convection in the zone where β_P>>1 (Fig. 3). This zone is wide in the case of the snowflake: the radius of the β_P =1 contour is, according to Eq. (1), of order of

$$r = r^* = a\beta_{pm}^{1/4}, \qquad (7)$$

where $\beta_{pm} \equiv 8\pi p / B_{pm}^2$ is the poloidal beta in the midplane. For the standard null, the size of the zone is significantly smaller, $r^* = a\beta_{pm}^{1/2}$. We assume that the pressure inside the scrape-off layer does not change appreciably between the midplane and the null-point region [33].

The velocity of the convective eddies (toroidally-symmetric rolls) can be evaluated from the following consideration. The effective gravity force per unit volume, associated with the toroidal curvature, is p/R; for the size of the zone lacking equilibrium r^*, the kinetic energy density acquired by the fluid element when crossing this zone is pr^*/R, yielding the characteristic element velocity of $\sqrt{pr^*/\rho R}$, where ρ is the plasma density. The characteristic turn-over frequency for a convective roll of size r^* will be then $\omega_{conv} \sim \sqrt{p/\rho r^* R}$. One can note in passing that ω_{conv} is of the same order of magnitude as the growth rate of the curvature-driven flute instability. Using the estimate for the sound speed $\mathrm{v}_s \sim \sqrt{p/\rho}$, one can estimate the turn-over frequency as $\omega_{conv} \sim \mathrm{v}_s / \sqrt{r^* R}$. On the other hand, the transit time of the unperturbed plasma flow in the vicinity of the null-point region is $\tau_{flow} \sim \left(a^2 / \mathrm{v}_s r^*\right)\left(B_T / B_{pm}\right)$. The product $\omega_{conv}\tau_{flow} \sim \left(a/r^*\right)^{3/2}\sqrt{a/R}\left(B_T / B_{pm}\right)$ is always very large compared to unity, meaning that the convection spreads the flowing plasma over the whole convection zone before the plasma reaches the target.

One therefore arrives at the following scenario for snowflake divertor operation in a steady-state mode: The plasma continuously diffuses across the separatrix to the SOL and flows along the open field lines to the divertor targets. In the area of a very high beta near the PF null, the plasma experiences intense convective spreading over a wide area of weak magnetic field that is connected to all four divertor legs (Fig. 3). The plasma flow continues along each leg to the divertor target. The magnetic flux intercepted by each leg corresponds to the distance $r \sim r^*$ from the null. When projected to the midplane SOL this flux corresponds to the distance $\Delta^* \sim a(r^*/a)^3 \sim a\beta_{pm}^{3/4}$ from the separatrix.

For a numerical example (Table 2) we consider an ITER-scale generic tokamak: R=5 m, a=2m, B_T=5 T, B_{pm}=0.8 T, with the SOL plasma parameters n=5×10^{13} cm^{-3}, T_e=T_i=50 eV, and the SOL width in the equatorial plane Δ=0.7 cm. We see that the distance Δ^* is indeed greater than the anticipated SOL width. In other words, the heat flux is distributed among four divertor legs, and in each leg the width of a plasma channel is significantly broader (by a factor ~ Δ^*/Δ) than it would be without convective spreading.

The convective spreading could exist for the standard X-point (standard null, SN) divertor as well, but it would encompass only a much narrower area near the null and, therefore, would not lead to any substantial spreading of the heat flux. The comparison of the two divertors is provided in Table 2. One sees that the broadening of the wetted area on the target characterized by the parameter Δ^* is significant for the snowflake and relatively insignificant for the standard divertor.

The eventual heat flux on the divertor target is also affected by the location of the target downstream of the PF null, the target tilt with respect to the poloidal field and, most importantly, by the attainment of detachment [12, 17, 18]. Experimentally, the detachment occurs more easily in the snowflake than in the standard divertor, possibly due to the stronger reduction of the pre-detachment heat flux and the larger wetted area [18]. Similar conclusions have been made in the FAST design study [10]. A large spreading of the heat flux by the aforementioned mechanism should be a favorable factor in facilitating plasma detachment.

6. Significant reduction of the target heating during ELMs

As pointed out in Ref. [32], the broadening of the wetted area and activating all 4 snowflake strike points has particularly strong effect on the reduction of the heat flux on the target plates during ELM events. This broadening is due to the transient pressure increase in the SOL after ejection of particles and heat from the core plasma during ELMs. Increased pressure, in turn, leads to the increase of the parameter β_{pm} and the corresponding increase of the size of the convection zone r^*. The area over which the heat is spread during the ELM can therefore be significantly larger than that during the inter-ELM stage.

Further reduction of the target surface temperature increase during an ELM is caused by the temporal dilation of the heat pulse [19]. The lengthening of the heat pulse is related to the larger connection length. Simulations with the UEDGE code that include both convective and conductive losses [19] indicate that this effect can be substantial. Delays in the arrival of the ELM heat pulse on the target plates have been experimentally observed on the TCV facility [34].

On large tokamaks, a non-negligible amount of the ELM energy can be delivered by weakly collisional fast electrons. Their propagation to the target, in the case of formation of the convection zone, may be affected by tangling of the poloidal field in the convective zone. No quantitative estimates of such an effect are, however, available at present.

7. The snowflake divertor for a power reactor

Based on the results presented in sections 5 and 6, one can suggest a hypothetical scheme for a snowflake divertor in a future power reactor. There is a variety of such reactors assessed over the years, from conventional modest-aspect-ratio tokamaks to spherical tori. For our conceptual

assessment we have chosen a more conservative version, with the same geometrical parameters as those mentioned in Sec. 5 and Table 2. For a 1 GW(e) fusion power plant, the exhaust power that will have to be accommodated inside the vacuum chamber will be W_{exh}~500 MW [2]. Of that, ~100 MW would be radiated from the fusion plasma and spread uniformly over the walls, so that divertor would have to accommodate the power W_{div}~400 MW. If the allowable power load per unit surface area on the divertor target is P, then the required wetted surface has to be W_{div}/P. To allow for some margin, we assume that P=5 MW/m^2, not 10 MW/m^2 considered usually as an upper bound for the manageable heat load. Then, the required surface area is 80 m^2.

We suggest using a divertor that would allow for the convective spreading of the plasma flow at some distance from the targets. This will then be a volume without internal barriers. The overall geometry of the targets would be as in Fig. 4. Assuming that convection spreads the heat uniformly between all four targets, we find that the width h of a wetted zone on each target has to be $h = (1/2\pi R)(W_{div}/4P)$, where the factor "4" in the denominator accounts for the presence of four strike points. For the aforementioned numerical parameters, this will be approximately 60 cm. A single divertor is envisaged, at the bottom of the confinement zone. The second divertor on the top would allow reduction of heat loads by an additional factor ~ 2, but we do not consider this option here.

The targets would be situated outside the convection zone, in the area where flux recompression begins, and the flow again acquires an organized form, as shown qualitatively in Fig. 4. The radius of the convective zone, as estimated in Sec. 5 and illustrated in Table 2, will be ~50 cm. Placing the targets at the distance 1.5 times further from the null-point would already make β_p on the targets ~ 1/5, i.e., significantly less than 1.

The distance of 75 cm from the PF null to the targets is sufficient to accommodate four target plates with the wetted zone of 60 cm on each of the plates. The poloidal field strength at the target, for $r=1.5r^*$, will be $2.25\beta_{pm}^{1/2}B_{pm}$. For the parameters of Table 2, this poloidal field will be $B_T/50$. Therefore, the ratio of B_p/B_T on the target which determines the intersection angle between the plate surface and the field lines, remains greater than 1 degree, and thus larger than the minimum value compatible with the technological limit from target plate alignment [35]. Detachment in the open SF divertor geometry has been studied on the NSTX facility and was found to occur easier than in the standard-null divertor due, probably, to a much stronger flux expansion. Numerical simulations mentioned in Sec. 5 seem to support this conclusion [10, 18]. The SF divertor is compatible with other techniques of the heat load mitigation, like impurity seeding [36].

Discussion above just delineates the possible characteristics of the snowflake divertor parameters. Further, more detailed studies should address issues of the optimum shape of the targets, location and structure of the pumping ports, helium pumping and other issues, to reach the level of detail even distantly approaching the one attained in the ITER divertor design [37].

8. Summary and discussion

The transition from a first-order magnetic null to a second-order null leads to profound changes in the plasma behavior in the divertor region. If one wants to identify the single most important cause of these changes, it is the formation of a large zone of a very weak poloidal magnetic field around the null point. The weak-field region leads to a variety of effects, some of which can control the plasma behavior inside the separatrix (like the increased magnetic shear and prompt ion losses from the pedestal region), whereas the other lead to significant decrease of the heat flux to the divertor outside the separatrix (strong convection spreading of the plasma, activation of four strike points, and temporal dilation of ELM heat flux). Many of these effects have been found in experiments on the NSTX and TCV experimental facilities.

Specifics of the snowflake divertor physics, when applied to a standard aspect ratio fusion reactor, favor a divertor without internal barriers that might hinder the convective spreading. Even for rather conservative assumptions regarding the allowable heat load (5 MW/m^2) the divertor may be relatively compact. It has to be emphasized that the PF coils for this divertor would be situated outside the TF coils.

For fusion facilities based on spherical tokamaks, a better configuration for the SF divertor could be geometrically open divertor without close-fitting side walls that could utilize the strong flux expansion at the divertor targets and an easier transition to detached regimes as discovered experimentally on the NSTX facility [11, 17].

Acknowledgments

The authors are grateful to Dr. V.A. Soukhanovskii for discussions of experiments on the NSTX facility at Princeton, and to Drs. B. Labit, H. Reimerdes, and W. Vijvers, for discussion of experiments on the TCV facility at Lausanne. These two spectacular experiments have been an inspiration to our work. We are grateful to Dr. L. Lodestro (LLNL) for helpful comments Work performed for U.S. DoE by LLNL under Contract DE-AC52-07NA27344.

References

[1] A. Loarte, B. Lipschultz, A. Kukushkin, G. Matthews, P. Stangeby, N. Asakura, G. Counsell, G. Federici, A. Kallenbach, K. Krieger, A. Mahdavi, V. Philipps, D. Reiter, J. Roth, J. Strachan, D. Whyte, R. Doerner, T. Eich, W. Fundamenski, A. Herrmann, M. Fenstermacher, P. Ghendrih, M. Groth, A. Kirschner, S. Konoshima, B. LaBombard, P. Lang, A. Leonard, P. Monier-Garbet, R. Neu, H. Pacher, B. Pegourie, R. Pitts, S. Takamura, J. Terry, E. Tsitrone, the ITPA Scrape-off Layer, and D. P. T. Group, "Chapter 4: Power and particle control," Nucl. Fusion **47**, S203 (2007).

[2] F. Najmabadi and the ARIES team. "Overview of the ARIES-RS reversed-shear tokamak power plant study." Fusion Eng. Des., **38**, 3 (1997).

[3] D.D. Ryutov. 'Geometrical Properties of a "Snowflake" Divertor.' Phys. Plasmas, **14**, 064502, June 2007.

[4] V.A. Soukhanovskii, H. Reimerdes and NSTX-U and TCV Research Teams. "Advanced Divertor Configurations with Large Flux Expansion." Paper I-12 at the Conference on Plasma-Surface Interactions, Aachen, May 2012; To appear in J. Nucl. Materials, 2012.

[5] A. Leonard, M. A. Mahdavi, S. L. Allen, N. H. Brooks, M. E. Fenstermacher, D. N. Hill, C. J. Lasnier, R. Maingi, G. D. Porter, T. W. Petrie, J. G. Watkins, and W. P. West, "Distributed divertor radiation through convection in DIII-D," Phys. Rev. Lett. 78, 4769, 1997. A. Leonard, M. A. Mahdavi, C. J. Lasnier, T. W. Petrie, P.C. Stangeby. "Scaling radiative divertor solutions to high power in DIII-D." Nucl. Fusion, **52**, 063015 (2012).

[6] T.W. Petrie, M.R. Wade, N.H. Brooks, M.E. Fenstermacher et al. "Compatibility of the radiating divertor with high performance plasmas on DIII-D." J. of Nucl. Mat., **363-365**, 416 (2007).

[7] M. Kotschenreuther, P. Valanju, S. Mahajan, and J. Wiley, "On heat loading, novel divertors, and fusion reactors," Phys. Plasmas **14**, 72502 (2007); P.M. Valanju, M. Kotschenreuther, S.M. Mahajan, and J. Canik, "Super-X divertors and high power density fusion devices." Phys.

Plasmas 16, 056110 (2009).

[8] D.D. Ryutov, R.H. Cohen, T.D. Rognlien, M.V. Umansky. "Magnetic field structure of a snowflake divertor." Phys. Plasmas, **15**, 092501 Sept. 2008.

[9] E. Mazzucato. "A midsize tokamak as a fast track to burning plasmas." AIP Advances **1**, 012101 (2011).

[10] V. Pericoli Ridolfini, R. Zagórski, G. Artaserse, G. Calabrò, F. Crisanti, G. Maddaluno, G. Ramogida and B. Viola. " Comparative study of a conventional and snowflake divertor for the FAST tokamak." Paper presented at PSI Conference, Aachen, May 2012; to appear in J. Nucl. Mat.

[11] Zheng GuoYao, Pan YuDon, Feng KaiMing, He HongDa, Cui XueWu. "Snowflake divertor simulation for HL-2M conception design." Paper P1-056 presented at the EPS Conf. on Plasma Physics, Stockholm, Sweden, July 2-6 2012.

[12] V. A. Soukhanovskii, J.-W. Ahn, R. E. Bell, D. A. Gates, S. Gerhardt, R. Kaita, E. Kolemen, B. P. LeBlanc, R.Maingi, M. Makowski, R. Maqueda, A.G. McLean, J. E. Menard, D. Mueller, S. F. Paul, R. Raman, A. L. Roquemore, D. D. Ryutov, S.A. Sabbagh, H. A. Scott. "Taming the plasma-material interface with the 'snowflake' divertor in NSTX," Nucl. Fus., **51**, 012001 January 2011.

[13] F. Piras, S. Coda, I. Furno, J.-M. Moret, R.A. Pitts, O. Sauter, B. Tal, G. Turri, A. Bencze, B.P. Duval, F. Felici, A. Pochelon, C. Zucca. "Snowflake divertor plasmas on TCV," Plasma Phys. Controlled Fusion, **51**, 055009 , May 2009.

[14] F. Piras, S. Coda, B.P. Duval, B. Labit, J. Marki, S.Y. Medvedev, J.-M. Moret, A. Pitzschke, O. Sauter, TCV Team. ""Snowflake" H Mode in a Tokamak Plasma," Phys. Rev. Lett., **105**, 155003 October 2010.

[15] F. Piras, S. Coda, B.P. Duval, B. Labit, J. Marki, S.Y. Medvedev, J.-M. Moret, A. Pitzschke, O. Sauter, TCV Team. "Snowflake divertor experiments on TCV." Plasma Phys. Controlled Fusion, **52**, 124010 December 2010.

[16] S. Coda for the TCV team**. "**Progress and scientific results in the TCV Tokamak." Nucl . Fusion, **51**, 094017, September 2011.

[17] V. A. Soukhanovskii, J.-W. Ahn, R. E. Bell, D. A. Gates, S. Gerhardt, R. Kaita, E. Kolemen, H. W. Kugel, B. P. LeBlanc, R.Maingi, R. Maqueda, A. McLean, J. E. Menard, D. M. Mueller, S. F. Paul, R. Raman, A. L. Roquemore, D. D. Ryutov, H. A. Scott. "'Snowflake' divertor configuration in NSTX." J. Nucl. Mat., **415**, S365 August 2011.

[18] V.A. Soukhanovskii, Ronald E. Bell , Ahmed Diallo , Stefan Gerhardt , Stanley M. Kaye, E Kolemen , Benoit P. LeBlanc , Adam McLean , J. E. Menard , Stephen F. Paul , Mario Podesta , R Raman , Thomas D. Rognlien , A. L. Roquemore , Dmitri D. Ryutov , F Scotti , M Umansky , D Battaglia , Michael G. Bell , David A. Gates , R Kaita , Rajesh Maingi , Steven A. Sabbagh. " Snowflake Divertor Configuration Studies in NSTX." Phys. Plasmas, **19**, to appear in August 2012.

[19] T.D. Rognlien, R.H. Cohen, D.D. Ryutov, and M.V. Umansky, "Comparison of ELM heat loads in snowflake and standard divertors," Proc. 20th Int. Conf. Plasma Surface Interactions, May 21-25, 2012, Aachen, Germany; submitted to J. Nucl. Mater.

[20] M.V. Umansky, R.H. Bulmer, R.H. Cohen, T.D. Rognlien. D.D. Ryutov. "Analysis of geometric variations in high-power tokamak divertors." Nuclear Fusion, **49**, 075005, July 2009.

[21] S. Yu. Medvedev, A. A.Ivanov, A. A. Martynov, Yu. Yu. Poshekhonov, R. Behn, Y. R. Martin, J-M. Moret, F. Piras, A. Pitzschke, A. Pochelon, O. Sauter, L. Villard**.** "Edge Stability and Pedestal Profile Sensitivity of Snowflake Diverted Equilibria in the TCV Tokamak," Contrib. Plasma Phys. **50**, 324 – 330, May 2010.

[22] M.V. Umansky, T.D. Rognlien, D.D. Ryutov, P. B. Snyder. "Edge Plasma in Snowflake Divertor," Contrib. Plasma Physics, **50**, 350, May 2010.

[23] S.Yu. Medvedev, A.A. Ivanov, A.A. Martynov, Yu.Yu. Poshekhonov,
Y.R. Martin, J-M. Moret, F. Piras, A. Pochelon, H.Reimerdes, O. Sauter, L. Villard and the TCV team. "Optimization of the snowflake diverted equilibria in the TCV tokamak." Paper P1-29 presented at the EPS Conf. on Plasma Physics, Stockholm, Sweden, July 2-6 2012.

[24] A. V. Chankin and G. M. McCracken, "Loss Ion Orbits at the Tokamak Edge." Nucl. Fusion 33, 1459 (1993).

[25] D.D. Ryutov, M.V. Umansky. "Ion Drifts in a Snowflake Divertor." "Phys. Plasmas," **17**, 014501, January 2010.

[26] C. S. Chang, S. Kue, and H. Weitzner, "X-transport: A baseline nonambipolar transport in a diverted tokamak plasma edge." Phys. Plasmas 9, 3884, 2002

[27] S. I. Krasheninnikov "On scrape-off layer transport." Physics Letters A, 283, 368 (2001).

[28] D.D. Ryutov, R.H. Cohen, I. Joseph, T.D. Rognlien, M.V. Umansky. The dynamics of coherent scrape-off layer structures in a snowflake divertor. Poster UP6.00119, APS DPP Annual Meeting, Dallas, TX, November 17-21 2008.

[29] D.D. Ryutov, M.A. Makowski, M.V. Umansky. "Local properties of the magnetic field in a snowflake divertor," PPCF, **52**, 105001, Oct. 2010.

[30] E. Kolemen, D.A. Gates, S. Gerhardt, C.W. Rowley, N.J. Kasdin, J. Kallman, V. A. Soukhanovskii, D. M. Mueller. "Strike point control for the National Spherical Torus Experiment (NSTX)," Nucl. Fusion, **50**, 105010, October 2010.

[31] J. Wesson. "Tokamaks" (2011)

[32] D. D. Ryutov, R.H. Cohen , T.D. Rognlien and M. V. Umansky. "Plasma convection near the magnetic null of a snowflake divertor during an ELM event." Contrib. Plasma Phys., **52**, No. 5-6, 539 – 543, June 2012.

[33] B. Lipschultz, X. Bonnin, G. Counsell, A. Kallenbach, A. Kukushkin, K. Krieger, A. Leonard, A. Loarte, R. Neu, R. Pitts, T. Rognlien, J. Roth, C. Skinner, J. Terry,

E. Tsitrone, D. Whyte, S. Zweben, N. Asakura, D. Coster, R. Doerner, R. Dux, G. Federici, M. Fenstermacher, W. Fundamenski, P. Ghendrih, A. Herrmann, J. Hu, S. Krasheninnikov, G. Kirnev, A. Kreter, V. Kurnaev, B. Labombard, S. Lisgo, T. Nakano, N. Ohno, H. Pacher, J. Paley, Y. Pan, G. Pautasso, V. Philipps, V. Rohde, D. Rudakov, P. Stangeby, S. Takamura, T. Tanabe, Y. Yang, and S. Zhu. "Plasma-surface interaction, scrape-off layer and divertor physics: implications for ITER" Nucl. Fusion **47**, 1189 (2007).

[34] B. Labit, G. Canal, H. Reimerdes, B. Tal, W. Vijvers, S. Coda, B.P. Duval, T. Morgan, G. De Temmerman, J. Zielinski and the TCV team, "Properties of Snowflake Diverted H-Mode Plasmas in TCV." Paper P5-091 presented at the EPS Conf. on Plasma Physics, Stockholm, Sweden, July 2-6 2012.

[35] A, S. Kukushkin. Private communication to D.R., 2007.

[36] V. A. Soukhanovskii, R. E. Bell, A. Diallo, S. Gerhardt, R. Kaita, S. Kaye, E. Kolemen, B. P. LeBlanc, R. Maingi, A. McLean, J. E. Menard, D. Mueller, S. F. Paul, M. Podesta, R. Raman, A. L. Roquemore, D. D. Ryutov, F. Scotti. "Divertor heat flux mitigation with impurity-seeded standard and snowflake divertors in NSTX." Paper P5-049 presented at the EPS Conf. on Plasma Physics, Stockholm, Sweden, July 2-6 2012.

[37] R.A. Pitts, A. Kukushkin, A. Loarte, A. Martin, M. Merola, C.E. Kessel, V. Komarov, M. Shimada. "Status and physics basis of the ITER divertor." Physica Scripta, T**138**, 014001 (2009).

Table 1 Conditions for an "approximate" snowflake to be close to an "exact" one.

Effect or parameter	Proximity constraint
Flux expansion; Connection length; Specific volume; Magnetic shear; Blob connectivity.	$D < D_{\exp ansion} \equiv a\left(\Delta / a\right)^{1/3}$
Prompt ion loss	$D < D_{prompt} \equiv a\varepsilon^{2/5};\ \varepsilon = \frac{\rho_i}{a}\frac{B_T}{B_{pm}}\sqrt{\frac{a}{R}}$
Plasma convection	$D < D_{\beta_p} \equiv r*$

Table 2. Comparison of the curvature-driven convection in a snowflake and in a standard divertor[a].

	Snowflake		Standard	
The size of a strongly convective zone	$D^*=a(\beta_{pm})^{1/4}$	*47 cm*	$D^*=a(\beta_{pm})^{1/2}$	*11 cm*
Turn-over time	$(\beta_{pm})^{1/8}(aR)^{1/2}/c_s$	*22 μs*	$(\beta_{pm})^{1/4}(aR)^{1/2}/c_s$	*11 μs*
Parallel transit time	$(B_T/B_{pm})\times(a/c_s)$ (a/D^*)	*760 μs*	$(B_T/B_{pm})\times(a/c_s)$	*180 μs*
Affected width projected to the midplane	$\Delta^*\sim a(D^*/a)^3$	*2.6 cm>Δ*	$\Delta^*\sim a(D^*/a)^2$	*6 mm <Δ*

[a] Device parameters: R=500 cm, a=200 cm, B_{pm}=5 T, B_{pm}=0.8 T; parameters of the midplane SOL: $n=5\times10^{13}$ cm^{-3}, $T_e=T_i$=50 eV, $\beta_{pm}\approx3\times10^{-3}$, $c_S=7\times10^6$ cm/s, Δ=0.7 cm.

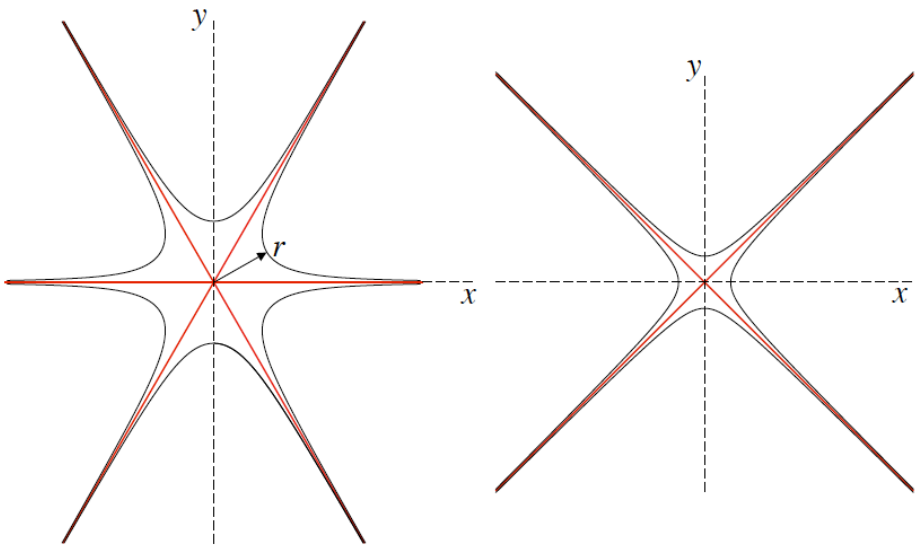

Figure 1. The shape of separatrix in the vicinity of the poloidal field null for the snowflake divertor (left) and standard divertor (right). Shown by a bold line is a separatrix; thin line represents an adjacent flux surface. The confinement region is in both cases situated in a sector pointing upward. Note that in the case of a snowflake there are four branches of the separatrix pointing downward, so that one can have four strike points in the divertor.

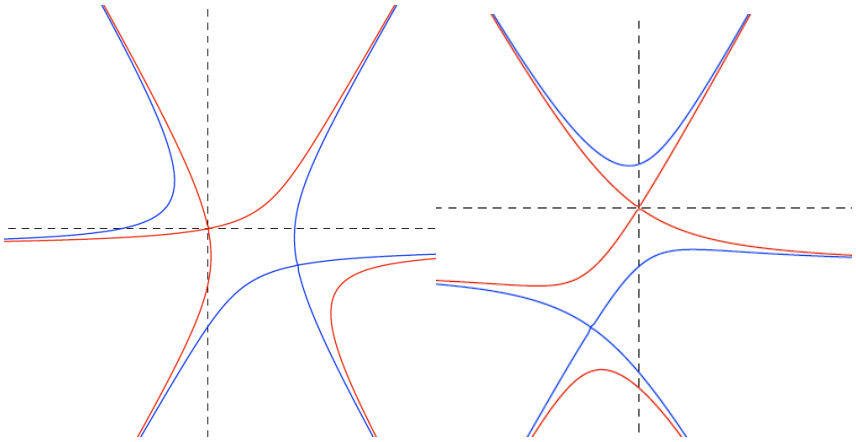

Figure 2. The snowflake-minus (left) and snowflake-plus (right) that appear instead of an exact snowflake if the currents in the divertor coil deviate from those needed to produce an exact snowflake. Two closely-spaced first-order nulls appear. Typically, if the current is lower (higher) than the "exact" value, a snowflake-minus (snowflake-plus) appear, whence the naming convention. In the snowflake-minus case, the secondary separatrix (blue) encloses the main one (red).

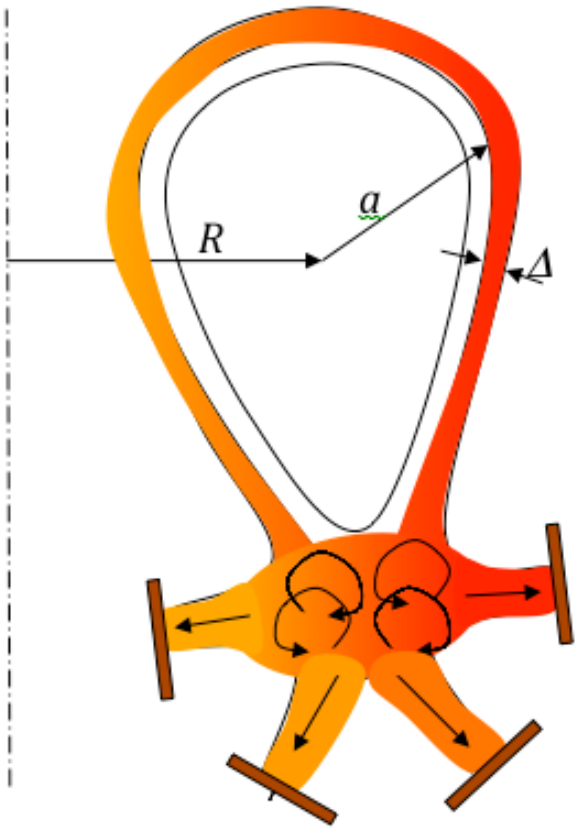

Figure 3. Convection driven by the toroidal curvature causes spreading of the plasma between all four strike points and broadening of the wetted area.

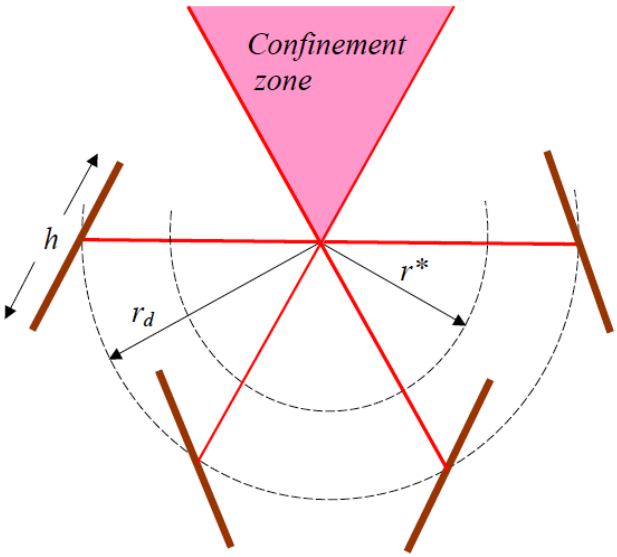

Figure 4. Schematic of a convective snowflake divertor. The radius r^* of a convective zone is 1.5 times smaller than the distance r_d from the null to the targets, meaning that β_p on the targets is approximately 0.2.